Measurement of Total Condensation on a Shrouded Cryogenic Surface using a Single Quart Crystal Microbalance

B. J. Haid, T. N. Malsbury, C. R. Gibson, C. T. Warren

June 27, 2008

Disclaimer

This document was prepared as an account of work sponsored by an agency of the United States government. Neither the United States government nor Lawrence Livermore National Security, LLC, nor any of their employees makes any warranty, expressed or implied, or assumes any legal liability or responsibility for the accuracy, completeness, or usefulness of any information, apparatus, product, or process disclosed, or represents that its use would not infringe privately owned rights. Reference herein to any specific commercial product, process, or service by trade name, trademark, manufacturer, or otherwise does not necessarily constitute or imply its endorsement, recommendation, or favoring by the United States government or Lawrence Livermore National Security, LLC. The views and opinions of authors expressed herein do not necessarily state or reflect those of the United States government or Lawrence Livermore National Security, LLC, and shall not be used for advertising or product endorsement purposes.

Measurement of Total Condensation on a Shrouded Cryogenic Surface using a Single Quart Crystal Microbalance

B.J. Haid, T.N. Malsbury

Lawrence Livermore National Laboratory, P.O. Box 808, Livermore, CA 94551

C.R. Gibson, C.T. Warren

General Atomics, P.O. Box 85608, San Diego, CA 92186

A single quartz crystal microbalance (QCM) is cooled to 18 K to measure condensation rates inside of a retractable "shroud" enclosure. The shroud is of a design intended to minimize condensate on fusion targets to be fielded at the National Ignition Facility (NIF). The shroud has a double-wall construction with an inner wall that may be cooled to 75-100 K.

The QCM and the shroud system were mounted in a vacuum chamber and cooled using a cryocooler. Condensation rates were measured at various vacuum levels and compositions, and with the shroud open or closed. A technique for measuring total condensate during the cooldown of the system with an accuracy of better than $1.0 \times 10^{-6} \text{g/cm}^2$ was also demonstrated. The technique involved a separate measurement of the condensate-free crystal frequency as a function of temperature that was later applied to the measurement of interest.

Introduction

The performance of a retractable cryogenic condensation shroud is assessed by measuring mass deposition using a commercial quartz crystal microbalance (QCM) that is operated at cryogenic temperature. This technique is applied to a shroud design that will enclose cryogenic targets to be fielded at the National Ignition Facility (NIF). NIF indirect drive (ID) ignition targets will contain frozen DT fuel to be driven to nuclear fusion by a ~1 megajoule laser shot. The targets will be operated at ~18K. The accumulation of cryo-condensate on the targets must be minimized as the condensate will disturb the laser light / DT fuel interaction and inhibit the drive to nuclear fusion. Therefore the cryostat that supports the target includes a retractable shroud to block residual gases in the vacuum chamber for up to 24 hr from the start of cooldown to a few seconds before the laser shot. Most of this duration involves creating a highly symmetrical spherical layer of DT fuel by precise control of the target temperature distribution. The maximum allowable condensate layer surface density on the target at the time of the laser shot is 1×10^{-5} g/cm^2.

An experimental system, shown in Figures 1-3, was built with a shroud geometry similar to the actual NIF target cryostat shroud. A QCM with an AT cut crystal was supported at the same location in the shroud that the ID target is held. The QCM is cooled to the nominal target temperature using a crycooler. The inner surface of the shroud is cooled to 75-100 K.

Quartz crystal microbalances have been demonstrated at cryogenic temperatures before to measure the accumulation of contaminants on cold surfaces[1-4]. They have also been used to measure condensation coefficients [5-7], gas absorption in substrates [8], and sublimation rates [9,10]. The accumulated mass density is inferred from the change in the crystal's shear-mode resonant frequency as measured by instrumentation that continuously excites the crystal. For sufficiently small mass accumulations (i.e < 0.0015 g/cm^2) the deposited mass per area m/A is given as:

$$\frac{m}{A} = K\left(f_0 - f_C\right) \tag{1}$$

where f_C is the measured crystal frequency, f_0 is the condensate-free crystal frequency, and K is a constant that is dependent on characteristics of the crystal.

K has a negligible dependence on temperature and therefore the QCM is easily applied for measuring deposition rate as long as the crystal temperature is maintained constant throughout the measurement. However, f_0 is strongly dependent on temperature. Therefore when measuring the total deposited mass the effect of temperature must be accounted for. For the QCM used in the system described here, the change in f_0 from room-temperature to 20K would lead to a deposition overestimate of ~8×10^{-5} g/cm^2 if the room-temperature f_0 is applied to an 18 K measurement.

In previous works, the temperature-induced error at cryogenic temperature was avoided by applying one of three methods. In all cases the QCM is maintained at constant temperature throughout the measurement. In the first method, the QCM provides a rate measurement without consideration of the total deposition thickness as an accurate rate measurement is obtained using the room-temperature K value [4-7]. For the second method the partial pressures of condensable gases are low enough during the cooldown to the measurement temperature to allow the assumption that the initial deposited mass is negligible [8,9]. In the third method, an additional "reference" QCM with the same crystal geometry is maintained at the measurement QCM temperature, but the crystal is within a sealed enclosure and assumed to remain free of deposition [1-3,10]. The condensate thickness is determined from the difference in resonant frequency between the two crystals.

The system described here uses a single commercial QCM system including a crystal, crystal holder, and instrumentation; but with additional instrumentation for measuring the quartz crystal temperature by a small ~3 mg resistance thermometer that is mounted directly to the crystal's edge. f_0 is strongly temperature-dependent, but if the relationship is repeatable then $f_0(T)$ may first be measured over the operating temperature range in an environment that causes negligible condensation. Total mass deposition in the actual test case is then calculated with Equation 1 while applying the crystal temperature to the predetermined $f_0(T)$ relation.

The shroud performance was tested in a vacuum chamber with a system to adjust and measure the residual gas composition. QCM measurements were first conducted with the shroud open to validate the measurement technique. In this configuration the mass deposition rate can easily be predicted from the vacuum measurement using the Hertz-Knudsen equation. Then the shroud was closed and measurements were performed with chamber pressures that are higher than expected for the actual NIF system. Finally, the QCM crystal temperature and resonant frequency were recorded over several cooldowns. Different cooldown temperature trends were obtained by applying electrical heating to the shroud and cold mount cooling paths. Cooldowns with the best achievable vacuum for this system were used to generate $f_0(T)$ for 18K<T<300K. A cooldown representative of the NIF system was then performed with a chamber pressure that is higher than expected. These measurements demonstrated a technique for verifying that the condensation on the target following an actual NIF system cooldown will be negligible.

Experimental Apparatus

The test shroud, shown in Figure 1, includes a double walled enclosure. The outer wall is maintained at room-temperature, and the inner wall may be cooled to within the range of 75-100K by the first stage of a two-stage GM cryocooler. Each wall contains two halves, such that the shroud may be opened by pulling the two halves apart as illustrated in Figure 1b. The shroud halves are mounted to two fiberglass arms, with each arm supporting both an inner and outer

half. The shroud opens in a clamshell form by rotating the arms about their axis that is set back 310 mm behind the QCM center. The opposite halves of the inner wall include overlapping edges to reduce gas conduction across their contact interface. The edges of the outer wall butt together when the shroud is closed. On the actual NIF crystoat the outer shroud includes a fluoroelastomer foam gasket bonded to one of the halves that creates a seal against the edges of the opposite half. In the test system, the seal is simulated using a low-outgassing tape. A 69 mm diameter room-temperature disk is located 5mm behind the base of the inner shroud wall. The disk simulates a "blast shield" that protects the cryostat from x-rays and debris generated by the laser shot.

The QCM is held within the shroud by a copper stalk that extends from a cold mount located behind the blast shield. The cold mount can be cooled to below 7K by the cryocooler second stage. The crystal surface faces the overlap between opposite shroud halves such that gas conduction that passes between the opposite halves will be captured on the crystal as much as any other location on the QCM assembly, leading to a conservative measurement. The stalk extends through a 16.5 mm hole at the center for the blast shield. To reduce gas conduction along the target stalk, a 17 mm square piece of copper sheet is mounted to the stalk and extends into a baffle feature that is bonded to the shroud inner wall. The gap between copper sheet faces and the inner shroud baffle is 1.7mm. The areas behind the blast shield are covered by superinsulation (not shown) to minimize heat load on the cold mount.

The ~3 mg resistance temperature sensor was bonded to the edge of the QCM crystal back-side using a thermally conductive epoxy as shown in Figure 2. The crystal is supported by leaf spring contacts that press it against the housing cover. The leaf spring contacts are electrically isolated from the main housing by a ceramic insert, and the cover is held in the main housing by a stainless steel spring.   These components provide poor conductance paths at cryogenic temperature. Therefore, a sufficient conductance was obtained be heat sinking the copper-sheathed miniature coaxial cable that comprises the last 78 cm of the electrical path connecting the QCM with its instrumentation. The miniature coax cable was wrapped several times at the cold mount end of the copper support and potted with a conductive epoxy. Stainless steel coaxial cable (not shown) joins the copper-sheathed coax with a room-temperature vacuum feedthrough. The stainless steel coax is heat sinked at an intermediate location to the cryocooler first stage.

A PID temperature controller drives an electrical heater located on the cold mount to maintain the crystal temperature at the controller setpoint. Electrical heaters are also used to maintain the blast shield and outer shroud wall at room-temperature, to adjust the steady-state inner shroud wall temperatures, and to vary cooldown rates.

The system is contained within a 3 m long, 1850 liter vacuum chamber. The shroud and QCM are supported near one end of the chamber as shown in Figure 3. The vacuum is monitored at this end of the chamber using an RGA and a separate ion gauge calibrated for nitrogen. The

chamber vacuum is maintained by a turbomolecular pumping system located at the opposite end of the chamber. The vacuum composition is adjusted by introducing gases through a leak valve located at the pumping end.

Results and Discussion

Condensation rates were measured by the QCM with the shroud open to test agreement with the rates predicted by the Hertz-Knudsen equation for the measured vacuum. In the first set of measurements, N_2 was leaked into the chamber to maintain a total pressure between 4.3×10^{-6} and 6.2×10^{-6} torr. The total pressure of all gases other than N_2 was less than 3.8×10^{-7} torr. The RGA measurement indicated that the gases with significant partial pressure include H_2O, N_2, O_2, He, and H_2.

The crystal temperature was stepped up through the range of 20-31 K. The solid curve of Figure 4 shows the rise in deposited mass relative to $t = 0$. The crystal temperature is indicated on the upper x-axis. The mass deposition predicted from the vacuum measurement is shown by the dashed curve. A condensation coefficient of 1 is applied for N_2, O_2, and H_2O regardless of the crystal temperature. The temperature of the incident gas molecules is assumed to be 293 K.

The measured mass accumulation rates versus temperature are compared to literature data for sticking coefficients and vapor pressure. When the temperature is less than ~25 K the prediction and QCM measurement agree within the repeatability specification for the ion gauge (5%), indicating that the condensation coefficient approaches unity. The agreement also supports the assumption that the QCM manufacturer specified K–value is accurate at 20 K. At higher temperature the measured rate drops below the prediction indicating reduction in the condensation coefficient and a rise in sublimation rate. The departure from unity is consistent with reference 11 which reports condensation coefficient as a function of surface temperature for an impinging gas temperature of 300 K. Between 27.5 and 28.0 K the condensation rate is balanced with the sublimation rate, and sublimation exceeds condensation at higher temperature causing the deposited mass to decline. The temperature where sublimation equals condensation is checked against reported condensation coefficients and vapor pressure for N_2 [11].

A second set of shroud open measurements was conducted while leaking H_2O into the chamber to determine the ion gauge N_2-relative sensitivity for H_2O. The total pressure was held steady at several values across the range $4.9 \times 10^{-7} - 8.7 \times 10^{-6}$ torr. The crystal temperature was maintained in the range 20-28 K. A relative sensitivity of 0.93 was found to correlate the vacuum measurement with the condensation rate measurement, which falls within with the range of values reported reference 12.

Having validated the QCM and vacuum measurement system, the shroud was closed and condensation rates were measured with partial pressures of H_2O and N_2 that far exceed the

expectations for the NIF chambers. The QCM was maintained at 18 K and the shroud inner wall was maintained within the range of 75-100 K. Figure 5 shows condensate mass versus time over 12 h periods for three different vacuum compositions. For the solid curve the chamber pressure was dominated by an H_2O partial pressure between 7.8×10^{-5} and 1.1×10^{-4} torr. A relatively low deposition rate of 3.5×10^{-9} g/cm^2h was measured. The shroud is very effective at preventing water from reaching the QCM because H_2O has a condensation coefficient of ~1 [7] and a vapor pressure below 1×10^{-13} torr [13] at the shroud temperature. For the dashed curve the chamber composition was dominated by a partial pressure of N_2 between 8.9×10^{-6} and 1.1×10^{-5} torr. A much higher deposition rate of 2.9×10^{-7} g/cm^2h is observed because N_2 will not condense at the shroud temperature, but it will condense at the QCM temperature for which the condensation coefficient is ~1 [11] and the vapor pressure is ~1×10^{-13} torr [13].

For the dash-dot curve air was leaked into the chamber and the total pressure was maintained between 1.1×10^{-5} and 2.5×10^{-5} torr. This test verifies that O_2 does not cause a significantly higher mass deposition rate than an equal N_2 partial pressure. Assuming that the deposition rate caused by a particular component is proportional to the partial pressure of the component outside of the shroud, the case of air can be compared to the case of nearly pure N_2 by dividing the deposition rate by the total pressure. The rate and pressures are averaged over the 12 h measurements to obtain 0.032 $g/cm^2h \cdot torr$ for air and 0.031 $g/cm^2h \cdot torr$ for N_2.

In the final series of measurements three QCM cooldowns from approximately room-temperature to below 20 K were performed to obtain the crystal's $f_0(T)$ characteristic and to measure the condensation mass on the QCM following a notional NIF cooldown trend. Figure 6 shows the three temperature trends. The solid and dashed curves involved cooling the QCM with the inner shroud wall temperature maintained below 150 K and the chamber pressure of 1×10^{-6} torr or less throughout the cooldown. If the frequency versus temperature curves between these cooldowns is repeatable then it indicates that the curves really correspond to the condensate-free crystal and do not include some component caused by a repeated buildup in condensation. If condensation was occurring during the cooldown then the difference in durations would lead to different condensate amounts and the frequency-temperature curves would not match.

Figure 7 shows the resonant frequency versus crystal temperature relations derived from each of the cooldowns. For the cooling trends with the inner shroud wall initially cold, the resonant frequencies are within agreement to within 14.4 Hz throughout the measurement, and to within 0.9 Hz at 18 K which is equivalent to 1.1×10^{-8} g/cm^2. This is less than 0.2% of the maximum allowable condensate for NIF ID targets, providing confidence that $f_0(T)$ can be repeatable within sufficient accuracy. The larger difference at higher temperature is likely due to error in the temperature measurement caused by the presence of a gradient as the crystal cools.

The dash-dot curves of Figures 6 and 7 represent a typical NIF cooldown where both the shroud and the QCM are initially at room-temperature. H_2O was leaked into the chamber to maintain a

pressure of 1.2×10^{-5} torr or higher. The resonant frequency versus temperature for the typical NIF cooldown is below the previous two trials by 40-60 Hz over the entire temperature range, equivalent to $\sim 6 \times 10^{-7}$ g/cm^2. The difference is fairly steady and therefore it is not likely caused by condensation during the cooldown but rather indicates limited repeatability of the $f_0(T)$ curve. A negligible amount of condensation for the NIF cooldown is expected because the shroud cools faster than the QCM until after the shroud reaches its final steady-state temperature. The shroud starts to capture H_2O vapor before the QCM is cold enough to condense H_2O and a negligible condensate deposition should be expected over the typical NIF cooldown.

The discrepancy with the NIF cooldown frequency vs temperature relation can be explained by a greater opportunity for disturbance to the crystal. The two cooldowns with the inner wall always cold were performed within a 35 hour period. The typical NIF cooldown began 40 hours after the first two were completed, and for the last 6.5 h before the NIF cooldown the inner shroud wall was at room-temperature. Possible disturbances during the long idle period include: the buildup of contaminants on the crystal surface while the inner shroud wall is warm, ambient vibrations repositioning the crystal in the QCM housing, and thermal contraction during warmup and cooldown causing crystal repositioning. Therefore, when measuring condensation for a specific cooldown trend, the best accuracy is likely obtained when the condensate-free crystal resonant frequency versus temperature is characterized shortly before or after the cooldown trend of interest.

Conclusions

The method of determining total condensate mass at cryogenic temperature as the difference in the crystal frequency with a predetermined condensate-free frequency at the same temperature has been shown to provide an accuracy of better than 1×10^{-6} g/cm^2. The accuracy is limited by the repeatability of the condensate-free frequency. The repeatability is dependent on conditions of the test environment, such as cleanliness and ambient vibration, and the duration between the determination of the condensate-free frequency and the measurement of interest.

Water contributes an insignificant amount of condensation because it is captured by the shroud. Other gases that are not captured by the 75-100K shroud but condense on the 18K target (N_2, O_2, CO, Ar) may be conservatively assumed to behave as N2 as it is likely to be the most mobile of these gases at temperatures below the shroud temperature. N_2 has a higher vapor pressure and its condensation coefficient approaches unity at the lowest temperature.

The condensate buildup during a NIF cooldown is insignificant until the target is cold enough to condense the lower triple point gases because the shroud cools faster than the target and blocks H_2O before the target will condense it. The target reaches a temperature low enough to condense other gases shortly before reaching a steady-state operating temperature. Therefore, the total condensate buildup during the shroud-closed portion of a NIF shot cycle may be estimated by the

duration the target is at operating temperature. Based on results for the test shroud, the condensate buildup is proportional to time and the pressure of lower triple point gases by the constant 0.032 g/cm^{2}h·torr. For the ~5s between the shroud opening and the laser shot, the condensation rate is accurately estimated using the Hertz-Knudsen equation while assuming a condensation coefficient of 1 for all condensable gases present.

References

1. Wallace DA, Wallace SA, "Use of a cryogenically cooled QCM in conjunction with a programmable data acquisition system to detect and examine accreted mass on the sensing crystal caused by environmental contamination." *Proceedings of the SPIE - The International Society for Optical Engineering*, vol.1165, 1989, pp. 424-31.

2. Belyaeva AI, Drozhzhin NV, Konovodchenko EV, Panin VV, Silaev VI, Soldatenkov VA, "Quartz microbalance for studying surface contamination in cryogenic devices." *Instruments and Experimental Techniques*, vol.36, no.4, pt.2, July-Aug. 1993, pp. 660-2.

3. Wood BE, Hall DF, Lesho JC, Uy OM, Dyer JS, Green BD, Galica GA, Boies MT, Silver DM, Benson RC, Erlandson RE, Bertrand WT, "QCM flight measurements of contaminant films and their effect on Midcourse Space Experiment (MSX) satellite optics." *SPIE-Int. Soc. Opt. Eng. Proceedings of the SPIE - The International Society for Optical Engineering*, vol.3124, 1997, pp. 34-40.

4. Baker MA, "Vacuum applications of the quartz crystal microbalance." *Vacuum*, vol.19, no.7, July 1969, pp. 327-330.

5. Baker MA, Holland L, "Use of a cooled quartz crystal microbalance to study the molecular flow and condensation of CO2 in vacuum." *Journal of Vacuum Science and Technology*, vol.6, no.6, Nov. 1969, pp. 951-4.

6. Levenson LL, "Condensation coefficients of argon, krypton, xenon, and carbon dioxide measured with a quartz crystal microbalance." *Journal of Vacuum Science and Technology*, vol.8, no.5, Sept.-Oct. 1971, pp. 629-35.

7. Bryson III CE, Cazcarra V, Chouarain M, and Levenson LL, "High-Precision Measurements of Condensation Coefficients. Results for Carbon Dioxide and Water Molecules." *Journal of Vacuum Science and Technology*, vol.9, no.1,Jan. 1972, pp. 557-560.

8. Seo Y, Yu I, "Adsorption of N_2 on a porous silica substrate studied by a quartz-crystal microbalance." *Physical Review B*, vol.60, no.24, Dec. 1999, pp. 17003-7.

9. Delval C, Rossi MJ, "Influence of Monolayer Amounts of HNO_3 on the Evaporation Rate of H_2O over Ice in the Range 179 to 208 K: A Quartz Crystal Microbalance Study." *Journal of Physical Chemistry A*, vol.109, 2005, pp. 7151-7165.

10. Boiziau C, Nuvolone R, "Sublimation du krypton à basse temperature." *Surface Science*, vol.38, 1973, pp.217-230.

11. Klipping G, Mascher W, "Production of vacuum by condensation on low temperature surfaces. II. The condensation of nitrogen and hydrogen on a defined cooled surface." Zeitschrift fur Angewandte Physik, vol. 16, no. 6, Dec. 1963. pp. 471-476.

12. Summers RL, "Empirical observations on the sensitivity of hot cathode ionization type vacuum gages." *NASA Technical Note*, NASA TN D-5285, Lewis Research Center, Cleveland OH, June 1969.

13. Honig RE, Hook HO, "Vapor pressure data for some common gases." *RCA Review*, vol. 21, no. 33, Sept. 1960, p. 360-368.

Figures

outer wall
(~293K)

inner wall
(75-100K)

baffle

QCM
(18-30K)

(a)

arm

blast shield
(~293K)

stalk and
mini-coax

cold mount
(≥7K)

(b)
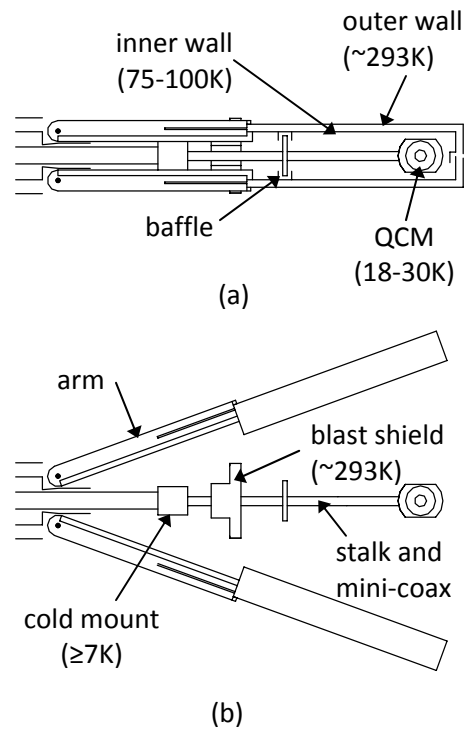
Figure 1: Shroud assembly and QCM geometry with (a) the shroud closed and (b) the shroud open. Section views are shown for the blast shield and shroud wall in (a). Not shown to scale.

cover

temperature
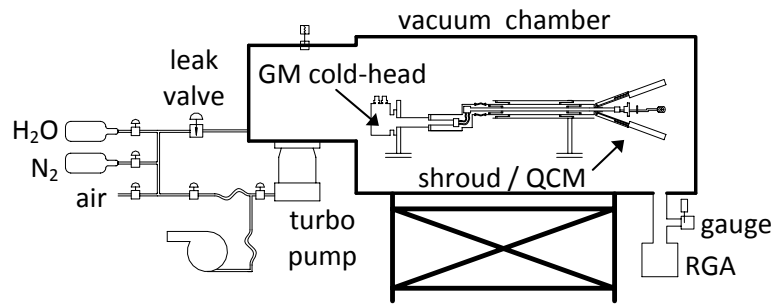sensor

crystal

contact

insert

crystal
back-side

housing
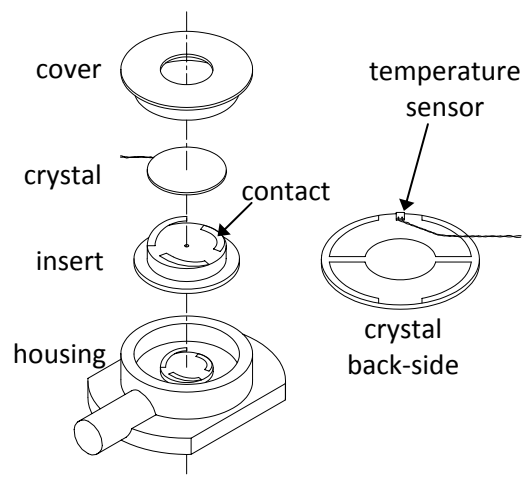
Figure 2: QCM assembly.

Figure 3: Layout of the vacuum system.
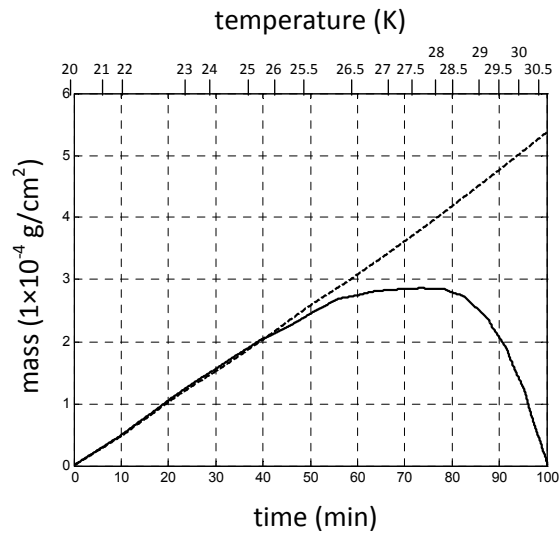
Figure 4: Measured (solid) and predicted (dashed) condensation rates with the shroud open while leaking N_2 into the chamber.
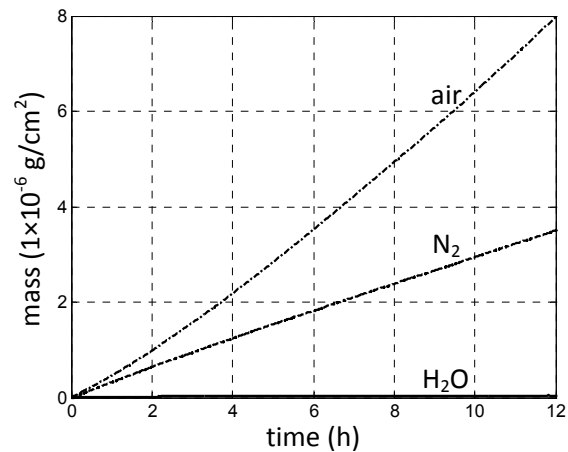
Figure 5: Rise in condensate mass with the shroud closed while leaking the indicated gases into the chamber.
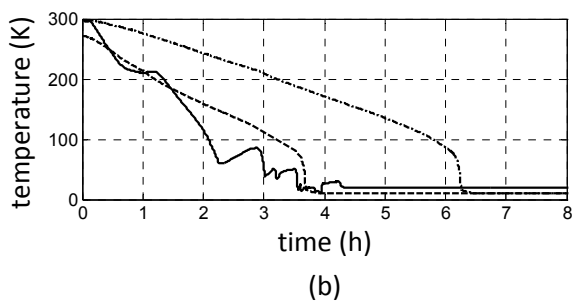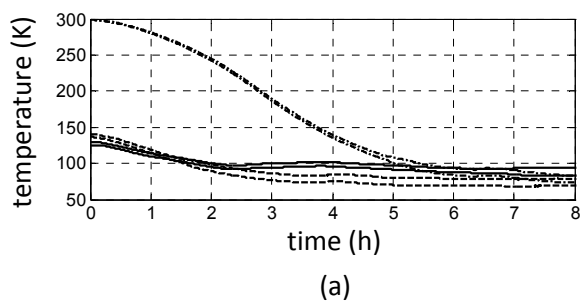

(a)

(b)

Figure 6: Three cooldown trends showing (a) the temperature of each shroud half and (b) the QCM temperature.
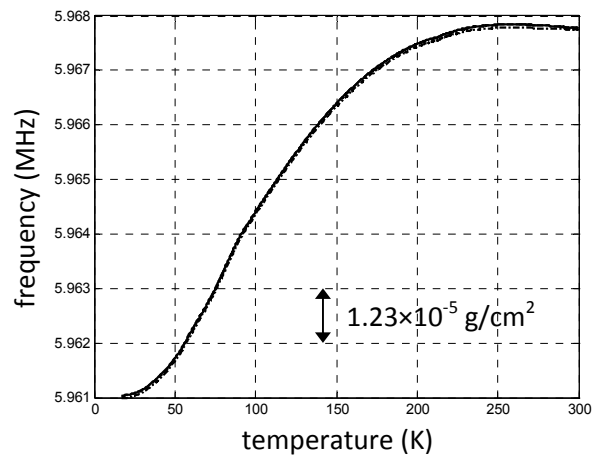
Figure 7: Condensate-free resonant frequency versus crystal temperature derived from each of the cooldowns of Figure 6.